



Published in final edited form as:

*Cell Host Microbe*. 2018 January 10; 23(1): 134–143.e6. doi:10.1016/j.chom.2017.12.002.

## Gut Microbes Egested During Bites of Infected Sand flies Augment Severity of Leishmaniasis Via Inflammasome-Derived IL-1 $\beta$

Ranadhir Dey<sup>1</sup>, Amritanshu B. Joshi<sup>1</sup>, Fabiano Oliveira<sup>2</sup>, Lais Pereira<sup>2,3</sup>, Anderson B. Guimarães-Costa<sup>2</sup>, Tiago D. Serafim<sup>2</sup>, Waldionê de Castro<sup>2</sup>, Iliano V. Coutinho-Abreu<sup>2</sup>, Parna Bhattacharya<sup>1</sup>, Shannon Townsend<sup>2</sup>, Hamide Aslan<sup>2</sup>, Alec Perkins<sup>2</sup>, Subir Karmakar<sup>1</sup>, Nevien Ismail<sup>1</sup>, Morgan Karetnick<sup>2</sup>, Claudio Meneses<sup>2</sup>, Robert Duncan<sup>1</sup>, Hira L. Nakhasi<sup>1</sup>, Jesus G. Valenzuela<sup>2,\*</sup>, and Shaden Kamhawi<sup>2,4,\*</sup>

<sup>1</sup>Laboratory of Emerging Pathogens, Division of Emerging and Transfusion Transmitted Diseases, Center for Biologics Evaluation and Research, Food and Drug Administration, Silver Spring, MD 20993, USA

<sup>2</sup>Vector Molecular Biology Section, Laboratory of Malaria and Vector Research, National Institute of Allergy and Infectious Diseases, National Institutes of Health, Rockville, Maryland 20852, USA

<sup>3</sup>Department of Molecular Microbiology and Immunology, Johns Hopkins Bloomberg School of Public Health, Baltimore, MD, 21205, USA

### SUMMARY

*Leishmania donovani* parasites are the cause of visceral leishmaniasis, and are transmitted by bite from phlebotomine sand flies. A prominent feature of vector-transmitted *Leishmania* is the persistence of neutrophils at bite sites, where they protect captured parasites leading to enhanced disease. Here, we demonstrate that gut microbes from the sand fly are egested into host skin alongside *Leishmania* parasites. The egested microbes trigger the inflammasome leading to a rapid production of IL-1 $\beta$ , which sustains neutrophil infiltration. Reducing midgut microbiota by pretreatment of *Leishmania*-infected sand flies with antibiotics, or neutralizing the effect of IL-1 $\beta$ , in bitten mice abrogates neutrophil recruitment. These early events are associated with impairment of parasite visceralization indicating that both gut microbiota and IL-1 $\beta$  are important for establishment of *Leishmania* infections. Considering that arthropods harbor a rich microbiota, its potential egestion after bites may be a shared mechanism that contributes to severity of vector-borne disease.

\*Correspondence: skamhawi@niaid.nih.gov or J.G.V. jvalenzuela@niaid.nih.gov.

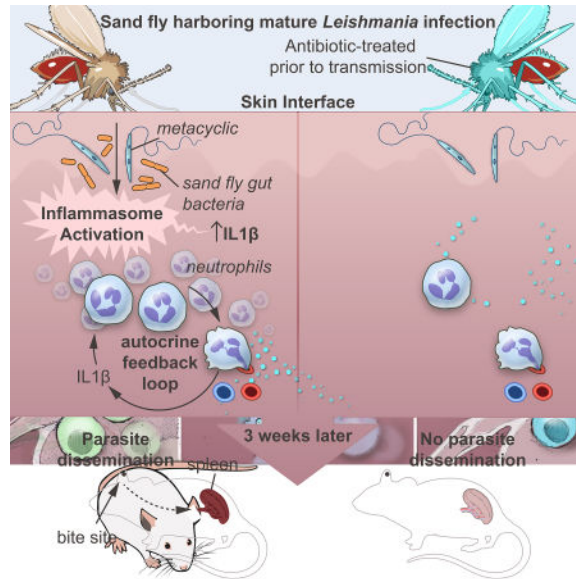
<sup>4</sup>Lead contact.

**Publisher's Disclaimer:** This is a PDF file of an unedited manuscript that has been accepted for publication. As a service to our customers we are providing this early version of the manuscript. The manuscript will undergo copyediting, typesetting, and review of the resulting proof before it is published in its final citable form. Please note that during the production process errors may be discovered which could affect the content, and all legal disclaimers that apply to the journal pertain.

### AUTHOR CONTRIBUTIONS

Conceptualization, R.D., F.O., J.G.V., and S.K.; Methodology, R.D., F.O., J.G.V., and S.K.; Investigation, R.D., A.B.J., F.O., L.P., A.B.G., T.D.S., W.C., P.B., I.V.C., S.T., H.A., A.P., Su.K., N.I. and M.K.; Resources, C.M., Ro.D.; Writing, R.D., F.O., H.L.N., J.G.V., and S.K.

## eTOC Blurb



Neutrophils recruited to sand fly bite sites shelter *Leishmania*, augmenting disease. Dey et al. demonstrate that egestion of sand fly gut microbiota into host skin primes the inflammasome to produce IL-1 $\beta$ , which sustains neutrophil recruitment. Removing gut microbiota or blocking IL-1 $\beta$  before transmission abolishes neutrophil recruitment and impairs *Leishmania* dissemination.

## INTRODUCTION

Vector-borne diseases account for over a billion new infections and more than a million deaths each year (WHO, 2014). Transmission of a variety of pathogens by bites of their arthropod vectors enhances pathogen establishment and disease severity (Cox et al., 2012; Liu and Bonnet, 2014; Peters et al., 2008; Pingen et al., 2016). Enhancement of disease following transmission of viruses by mosquitoes (Pingen et al., 2016) or *Leishmania* parasites by sand flies (Peters et al., 2008) has been associated to neutrophil-driven inflammation. Neutrophils are first responders to sites of skin injury and are a vital part of wound healing (de Oliveira et al., 2016). Therefore, their arrival at the bite site is partly driven by tissue damage caused by insect probing and biting. Yet mosquito or sand fly bites augment the response of neutrophils with consequences for pathogen establishment (Peters et al., 2008; Pingen et al., 2016). However, the mechanism driving sustained recruitment of neutrophils after vector bites has not been fully elucidated. Leishmaniasis, a vector-borne disease transmitted by bites of phlebotomine sand flies, encompasses a spectrum of diseases that range from self-healing cutaneous leishmaniasis (CL), to disseminating visceral leishmaniasis (VL). VL caused by *Leishmania donovani* in the Indian subcontinent and East Africa has a high fatality rate in untreated patients with patent infections. Following natural transmission by sand fly bites, *L. donovani* parasites migrate from the skin to the liver and spleen damaging organs, yet mediators of parasite dissemination from the bite site remain unknown.

Several vector-derived components, of insect and parasite origin, including saliva, proteophosphoglycans and exosomes, are regurgitated into the bite site and modulate the host immune response in favor of parasite survival (Atayde et al., 2015; Gomes and Oliveira, 2012; Rogers, 2012). Using a VL mouse model of vector-transmitted *L. donovani*, our data indicate that sand fly gut microbes are egested into host skin where it triggers the inflammasome and amplifies IL-1 $\beta$  production by neutrophils. IL-1 $\beta$  then acts as an early autocrine signal to sustain an intense recruitment of neutrophils to bite sites. Further, we show that the microbe-initiated immune response sanctions downstream events that govern dissemination of *L. donovani*.

## RESULTS

### Vector-transmitted *L. donovani* disseminates from the skin to the spleen

Twenty *L. donovani*-infected sand flies harboring transmissible infections (Figure S1A) reproducibly transmit about  $10^3$ – $10^4$  parasites to mice ears (Figure 1A; Figure S1B). A mean  $\pm$  SD of  $7.14 \pm 4.47$  *L. donovani* fed flies per ear (Figure S1C) result in parasite dissemination from the skin to the spleen by five weeks after vector-transmission (Figure 1B). After 30 weeks, 18/23 mice had splenic parasites, with a geometric mean  $\pm$  SD of  $3.98 \times 10^3 \pm 5,506$  parasites per spleen in positive mice. In contrast,  $10^5$  culture-derived metacyclics injected intradermally fail to visceralize (Figure 1B) affirming the heightened severity of vector-transmitted leishmaniasis.

Next, we explored the early innate immune response after a *L. donovani*-infected sand fly bite (IS), an uninfected sand fly bite (US), intradermal co-inoculation of *L. donovani* parasites and salivary gland sonicate (LG), or intradermal *L. donovani* injection (LI) from 3h up to 48h. Immunohistochemical (IHC) analysis of ear sections and flow cytometry gated on neutrophils and inflammatory monocytes (Figure S2A) recovered from ear cells established the intense and persistent nature of neutrophil recruitment to bite sites up to 48h following IS or US, compared to a weak and transient infiltration after LG or LI (Figure 1C–1E), reproducing findings following vector-transmission of *L. major* (Peters et al., 2008). Though neutrophil recruitment was generally similar after IS and US, it was significantly higher at 18h after IS (Figure 1C and 1E), potentially due to parasites or to the promastigote secretory gel (PSG) and exosomes, both reported to attract neutrophils (Rogers, 2012; Silverman and Reiner, 2011). Monocyte recruitment was not observed up to 6h (Data not shown), but was significantly higher at 18h after IS compared to LG and LI (Figure 1F). Interestingly, the number of recruited neutrophils and inflammatory monocytes per ear after IS compared to US was augmented by correcting for fed flies, becoming significant for monocytes at 18h (Figure S2B). Generally, US are unhampered by infection with *Leishmania* and tend to feed more easily.

Another striking difference among the groups was a significant increase in the number of degranulated mast cells 3h after IS compared to US, LG and LI, with US inducing an intermediate response (Figure 1G; Figure S2C and S2D). Mast cells release mediators that promote and qualify the innate immune response and have been implicated in production of CXCL1 and matrix metalloprotease 9 (MMP9) and the early recruitment of neutrophils (Chiba et al., 2015; De Filippo et al., 2013).

At the transcriptional level, CXCL1 and CCL2 chemokines, critical for recruitment of neutrophils and monocytes, respectively (De Filippo et al., 2013; Shi and Pamer, 2011), several markers of alternatively activated M2 monocytes/macrophages (Mo/M $\Phi$ ) (Murray and Wynn, 2011; Porta et al., 2009; Sica et al., 2014), associated to wound healing and the inability to kill *Leishmania* parasite (Murray and Wynn, 2011; Rogers, 2012), and the cytokines IL10 and IL1 $\beta$  were expressed at significantly higher levels after IS compared to LG and LI (Figure 1H and 1I). Interestingly, MMP9 was induced at significantly higher levels after IS compared to all other groups (Figure 1H and 1I). Apart from digestion of the extracellular matrix, MMP9 has been associated to intense recruitment of neutrophils (Bradley et al., 2012) and orchestrating a positive feedback loop for neutrophil recruitment to sites of inflammation (Opdenakker et al., 2001).

### Infected sand fly bites activate the NLRP3 inflammasome

Of pivotal significance, the sustained high induction of IL1 $\beta$  at 3h to 18h after IS and US compared to LI (Figure 1H and 1I) suggested that infected and uninfected sand fly bites may activate the inflammasome (Guo et al., 2015). A parallel induction of higher levels of TNF $\alpha$ , NOS2, and IFN $\gamma$  after IS compared to LG and LI (Figure 1H) further supported our hypothesis (Guo et al., 2015; Lima-Junior et al., 2013).

IL1 $\beta$  is tightly regulated at the transcriptional and translational levels, and by proteolytic processing (Guo et al., 2015; Radwan et al., 2010). To understand the biological relevance of IL1 $\beta$  induction after sand fly bites, we assessed its protein levels in ear tissue lysates at 6h after IS and US. Unexpectedly, the IL1 $\beta$  protein level was significantly higher after IS compared to US (Figure 2A). This was supported by IHC staining directed against mature soluble IL1 $\beta$  (Figure 2B). Notably, neutrophils were the main source of IL1 $\beta$  in mice ears at 6h after IS and showed a 37-fold increase in their number compared to resting skin (Figure 2C–E). Six hours after bites, the protein levels of NLRP3, pro-caspase1 and cleaved caspase1 were also reduced after US compared to IS (Figure 2F, Table S1). Importantly, after immunoprecipitation using apoptosis-associated speck-like protein containing a CARD domain (ASC), NLRP3 detection was considerably stronger after IS compared to US (Figure 2G, Table S1) signifying a more efficient assembly of the inflammasome after IS. Consistent with these conclusions, NLRP3 expression was significantly higher while expression of IFN $\beta$ , an inhibitor of the NLRP3 inflammasome (Guarda et al., 2011; Guo et al., 2015), was reduced after IS compared to US over the timeline of the study (Fig. 2H). Apoptotic cells that contribute to inflammasome activation (Shimada et al., 2012) and promote an anti-inflammatory environment (Ribeiro-Gomes and Sacks, 2012) were also more prevalent in ear sections after IS compared to US (Figure 2I).

Since *Leishmania* species have been reported to activate the NLRP3 inflammasome (Charmoy et al., 2015; Gurung et al., 2015; Zamboni and Lima-Junior, 2015), we incubated lipopolysaccharide (LPS)-primed bone marrow-derived macrophages (BMDM) with stationary-phase *L. donovani* parasites. High levels of mature IL1 $\beta$  were only produced in the presence of LPS, while parasites alone induced IL10 production (Figure 2J). Nevertheless, increasing the number of parasites incubated with presence of LPS-primed

cells significantly elevated IL1 $\beta$  secretion (Figure 2J) indicating that *Leishmania* contributes to activation of the inflammasome.

### **Gut-residing microbes are co-egested alongside *Leishmania* parasites during infected sand fly bites**

Induction of high levels of IL1 $\beta$  after IS and US led us to hypothesize that midgut microbes, reported from wild-caught and colonized sand flies (Kelly et al., 2017; Monteiro et al., 2016; Sant'Anna et al., 2012), may be inoculated into host skin. To demonstrate the egestion of midgut microbes during sand fly bites, we exposed infected flies to warmed sterile LB agar plates for 1h (Video S1), and allowed the bacteria to grow overnight (Figure 3A). We amplified *Leishmania* DNA from eight screened colonies, providing us with a definitive guide to bite sites (Figure 3B). We then isolated and sequenced bacteria from the *Leishmania*-positive bite sites and from plated midgut colonies of the sand flies (Figure 3C and 3D). Of the genera identified from bite sites, *Tsukamurella*, *Lysinibacillus*, *Paenibacillus*, *Solibacillus* and *Bacillus* were present in midgut colonies of sand flies used in probing. Importantly, *Tsukamurella* is also an indicator species that distinguishes microbiota of infected from uninfected midguts (Kelly et al., 2017).

### **Gut microbes of sand flies provide the initial signal for NLRP3 priming**

To demonstrate that midgut microbes prime the inflammasome, we provided sand flies harboring mature infections with a sugar meal containing an antibiotic cocktail for 36h after confirming that it has no adverse effect on the growth or differentiation of *Leishmania* parasites in culture (Figure S3A and 3B). We then demonstrated the efficacy of antibiotic treatment *in vivo* through its significant reduction of the number of cultivable gut microbiota (Figure 4A). We also demonstrated that sand flies given antibiotics were similar to controls in their survival (Figure 4B), their support of *Leishmania* growth and differentiation to infective metacyclics (Figure 4C), the virulence of their midgut-resident metacyclics, assessed by their ability to invade and replicate within bone marrow-derived macrophages (Figure 4D and 4E), their feeding behavior (Figure 4F) and their capacity to transmit parasites to mice ears (Figure 4G).

Diminishing gut microbiota by antibiotic-treatment had a significant effect on decreasing the IL1 $\beta$  protein level after bites compared to controls (Figure 4H). Additionally, protein levels of NLRP3, pro-caspase1 and cleaved caspase1 as well as IL1 $\beta$  were reduced in skin exposed to antibiotic-treated sand flies compared to controls (Figure 4I, Table S1). Furthermore, NLRP3 levels after immunoprecipitation with ASC were strongly decreased after antibiotic treatment (Figure 4J, Table S1) indicative of the loss of inflammasome assembly. Noteworthy, a prolonged treatment of uninfected sand flies using a stronger antibiotics cocktail also reduced IL1 $\beta$  and NLRP3 mRNA expression, and IL1 $\beta$  protein levels, compared to controls (Figure S3C and S3D) despite unaltered fitness of the flies (Figure S3E and S3F). These results provide a strong evidence of the role of gut microbes in initiating a potent inflammatory response by their rapid priming of the NLRP3 inflammasome.

## Inflammasome-derived IL1 $\beta$ augments neutrophil recruitment and its absence disrupts the establishment of *Leishmania* infection

To assess the relevance of gut microbiota or inflammasome-derived IL1 $\beta$  to *L. donovani* infection, we used antibiotic-treated sand flies to transmit parasites to mice, or treated mice with anakinra, an IL1R antagonist, prior to parasite transmission with untreated infected sand flies (Figure 4K–N). Due to the focal nature of sand fly bite sites – distinct focal sites of inflammation are visible along the ear section - we used IHC staining to accurately assess the effect of the two treatments on neutrophil recruitment. Both antibiotic treatment of infected sand flies or anakinra treatment of mice abrogated the intense recruitment of neutrophils observed in control mice 6h after infected sand fly bites (Figure 4K and 4M). Though we did not track the fate of the parasites at the bite site, both treatments also resulted in a significant decrease in the splenic parasite burden at three weeks after infection, an early timepoint chosen to assess parasite dissemination from the skin (Figure 4L and 4N). Interestingly, the intradermal co-injection of parasites with either 10<sup>3</sup> live *Solibacillus* bacteria (LI+CFU), recovered from a *Leishmania*-positive bite site (Figure 3C), or 1  $\mu$ g of LPS (LI+LPS) only partially reproduced the immune response after IS (Figure S4). Six hours after co-injection, both NLRP3 and IL1 $\beta$  were induced to significantly higher levels in mice co-injected with either LI+CFU or LI+LPS compared parasites alone (LI) (Figure S4A) leading to enhanced neutrophil recruitment (Figure S4B). However, expression of YM1, used as an indicator for M2 Mo/M $\Phi$ , and MMP9, uniquely induced by IS, (Figure 1H and 1I) remained low (Figure S4A), and parasite visceralization to the spleen three weeks later was poor (Figure S4C). These data demonstrate that alone, microbe-triggered inflammasome activation and IL1 $\beta$  production, though required, are insufficient for parasite dissemination, and emphasize the need for other components in the infectious inoculum to initiate the unique inflammatory response observed after IS.

## DISCUSSION

The early events governing pathogen establishment at bite sites of arthropod vectors are poorly investigated despite evidence that disease is often enhanced after vector-transmission (Liu and Bonnet, 2014; Peters et al., 2008; Pingen et al., 2016). This has mostly been attributed to immunomodulatory components of saliva co-egested with the pathogen into the host (Abdeladhim et al., 2014; Liu and Bonnet, 2014; Schmid et al., 2016). Recent studies have suggested that elements other than saliva may also participate in disease-enhancing features of pathogen-transmission by vector bites (Peters et al., 2008; Pingen et al., 2016). Our findings suggest that microbes residing in the gut of the sand fly are egested into the host alongside *Leishmania* and primes the inflammasome to produce significantly higher levels of IL1 $\beta$  compared to levels induced by parasites alone. Though *Leishmania* parasites have been reported to activate the inflammasome, this phenomenon has only been demonstrated in the presence of LPS (Charmoy et al., 2015; Lima-Junior et al., 2013). Here, we propose that microbes of the arthropod vector are providing the priming signal needed for optimal inflammasome activation in the natural setting of infected vector bites. We theorize that this early burst of microbe-induced IL1 $\beta$  provides an autocrine signal for further recruitment of neutrophils following vector-transmission of *Leishmania* amplifying the response. Of note, sand flies harboring mature *Leishmania* infections exhibit altered

feeding behavior with prolonged probing and increasing feeding persistence (Rogers, 2012). This can potentially lead to more cell damage at the bite site. As such, the higher levels of mature IL1 $\beta$  observed after infected sand fly bites could partly involve extracellular processing of immature IL1 $\beta$  by neutrophil and mast cell-derived proteases (Afonina et al., 2015; Opendakker et al., 2001). Indeed, mast cell degranulation, infiltration of neutrophils and MMP9 induction were all significantly higher after infected compared to uninfected sand fly bites.

The intensified and prolonged recruitment of neutrophils after bites of *L. donovani*-infected sand flies resembles the response described following bites of *L. major*-infected *Ph. duboscqi* (Peters et al., 2008). Since loss of neutrophils also significantly compromises *L. donovani* infection, we theorize that, similar to *L. major* (Peters et al., 2008), neutrophils likely play a part in shielding *L. donovani* parasites and promoting infection of macrophages post-transmission.

Increased recruitment of neutrophils was also observed following bites of virus-infected mosquitoes (Pingen et al., 2016). Importantly, this response led to enhanced viral establishment and dissemination caused by the enriched number of virus-susceptible myeloid cells arriving at the bite site. In the present study, a remarkably similar effect was observed for vector-transmitted *L. donovani*. After infected sand fly bites, successful dissemination of parasites to internal organs was associated to an intensified and prolonged recruitment of both neutrophils and inflammatory monocytes to the bite site. This led us to hypothesize that microbe-mediated enhancement of the inflammatory response, through its activation of the inflammasome, facilitate downstream events that govern parasite dissemination to internal organs. A significant reduction in parasite burden following transmission by antibiotic-treated infected sand flies, that was also associated to a poor infiltration of neutrophils, supports this hypothesis. It is important to underscore, however, that microbe-mediated neutrophil recruitment, though required, is not directly responsible for parasite dissemination. Whether microbes are involved in governing the early response to infected mosquito bites remains to be proven. However, the documented presence of bacteria in salivary glands of several mosquito species (Sharma et al., 2014; Tchioffo et al., 2015), combined with the fact that multiple pathogens are transmitted in saliva after they colonize the salivary glands, suggests that this may be possible.

Skin represents the first barrier against invading pathogens. Once breached, skin cells of the epidermis and dermis collaborate to release an array of mediators aimed at tissue repair and healing. This universal innate response involves sequential steps that are fine-tuned to produce a self-limiting inflammation involving a transient recruitment of neutrophils and monocytes to the site of injury, aimed at clearing damaged cells and foreign invaders and initiating tissue remodeling and wound repair (de Oliveira et al., 2016; Murray and Wynn, 2011). Considering that most arthropod vectors contain a rich microbial community in several tissues including the gut and salivary glands, and some such as ticks transmit several bacteria of medical importance (Berggoetz et al., 2014; Monteiro et al., 2016; Qiu et al., 2014; Sant'Anna et al., 2012; Sharma et al., 2014), vector-borne pathogens may have evolved mechanisms to enhance recruitment neutrophils and monocytes, the main cellular arms of this response (Peters et al., 2008; Pingen et al., 2016).

Microbial communities of vectors may vary according to environment and biotope, and the relevance of microbial diversity in induction of the inflammasome needs to be addressed. However, since a wide range of bacterial species efficiently prime the promiscuous NLRP3 inflammasome (Guo et al., 2015), we theorize that variations in microbial communities may have more of a quantitative than a qualitative effect on its activation potentially influencing severity of disease. We, therefore propose that the mechanism put forward here for the sustained recruitment of neutrophils is a central one that occurs in most if not all events that follow *Leishmania*-infected sand fly bites, and potentially bites of other infected vectors.

In summary, our collective data show that vector-transmission of *Leishmania* parasites initiates a unique sustained immune response at the bite site. We reveal a mechanism triggered by midgut microbiota that acts during the early hours after infected bites impacting the course of infection. Our data indicate that midgut microbes are egested during infected sand fly bites and initiate an early proinflammatory response via inflammasome activation and IL1 $\beta$  production that is necessary for intense and sustained recruitment of neutrophils to the bite site. Further, we show that this early inflammatory response facilitates downstream events that govern successful visceralization of *L. donovani* parasites. As such these early responses, occurring only following vector-transmission of parasites, promote the establishment of leishmaniasis. This puts a renewed emphasis on the importance of vector sand flies in pathogenesis of leishmaniasis, and the assessment of the efficacy of vaccine candidates. Importantly, the significance of vector microbiota likely transcends sand flies and leishmaniasis with analogous ramifications for other vector-borne diseases.

## STAR METHODS

### CONTACT FOR REAGENT AND RESOURCE SHARING

Further information and requests for resources and reagents should be directed to and will be fulfilled by the Lead Contact, Shaden Kamhawi (skamhawi@niaid.nih.gov).

### EXPERIMENTAL MODEL AND SUBJECT DETAILS

**Mice**—Six- to eight-week-old female BALB/c mice from Jackson Laboratories were used in experiments. Animals were housed under pathogen-free conditions at the NIAID Twinbrook animal facility in Rockville, MD. Animal group sizes were based on historical studies suitable for observing the effects of vector-transmitted and needle-initiated *Leishmania* infections. Animals were randomly assigned to groups exposed to *Leishmania*-infected sand flies, uninfected sand flies, or chosen for needle injection of parasites with or without salivary glands. All samples were assayed collectively so that the investigator was blind to the specific outcome of an assay for a particular group. All animal experimental procedures were reviewed and approved by the National Institute of Allergy and Infectious Diseases (NIAID) Animal Care and Use Committee under animal protocol LMVR4E. The NIAID DIR Animal Care and Use Program complies with the Guide for the Care and Use of Laboratory Animals and with the NIH Office of Animal Care and Use and Animal Research Advisory Committee guidelines. Detailed NIH Animal Research Guidelines can be accessed at <https://oma1.od.nih.gov/manualchapters/intramural/3040-2/>.



**Parasites**—The parasite strain used in this study, *L. donovani* (MHOM/SD/62/1S), was maintained by serial passages in Golden Syrian hamsters. *L. donovani* promastigotes were cultured in Schneider's medium (Gibco-BRL, NY) supplemented with 20% heat-inactivated fetal bovine serum, 2 mM L-glutamine, 100 U/mL penicillin, and 100 µL/mL streptomycin at 26°C.

**Sand flies**—*Lutzomyia longipalpis* sand flies, Jacobina strain, were reared at the Laboratory of Malaria and Vector Research, NIAID, NIH according to protocols provided in "Care and Maintenance of Phlebotomine Sand flies" (Lawyer et al., 2016).

## METHODS DETAILS

**Sand fly infections**—Two to four-day-old colony-bred *Lu. longipalpis* females were infected by artificial feeding through a chick membrane on defibrinated rabbit blood (Spring Valley Laboratories, Sykesville, MD) containing  $5 \times 10^6$  amastigotes of *L. donovani* and 30µl penicillin/streptomycin (10,000 units penicillin/10mg streptomycin) per mL of blood. It is important to note that *L. donovani* amastigotes were isolated from terminally sick hamsters with advanced visceral leishmaniasis (VL), and amastigotes were freshly prepared on the day of infection. Though not required, using fresh parasites from terminally sick hamsters in a VL model of infection reduces the variability during the development of *Leishmania* in individual sand flies. This produces more homogenous mature infections that are optimal for transmission experiments. Fully blood-fed female sand flies were separated and maintained at 26°C with 75% humidity and were provided 30% sucrose until the flies developed a mature infection for transmission.

**Antibiotic treatment of sand flies**—For antibiotic treatment of uninfected sand flies, females were fed on defibrinated rabbit blood for 3h in the dark. Fully blood-fed females were separated and maintained at 26°C with 75% humidity for 11 days. After separation, half of the blood-fed sand flies were offered a 30% sucrose solution containing 100U/ml Penicillin, 50µg/ml Gentamicin, 20µg/ml Vancomycin, 16µg/ml Doxycycline and 4µg/ml Clindamycin through soaked cotton balls. The second half was offered 30% sucrose. Dead sand flies were removed and counted every three days. For infected sand flies, females were given a weaker antibiotic cocktail of 100U/ml Penicillin, 50µg/ml Gentamicin and 4µg/ml Clindamycin for 36h after the development of mature transmissible infections (on days nine through 11 post-infection). The total parasite load per midgut and percent metacyclics were determined for antibiotic-treated and control sand flies by hemocytometer counts.

**Pre-transmission scoring**—The parasite load and percentage of metacyclics per midgut in *L. donovani*-infected sand flies were scored on the day of transmission. Depending on fly availability, 10–20 flies were anesthetized with CO<sub>2</sub>, washed in 5% soap solution and rinsed in 1X PBS prior to dissection. Each midgut was macerated with a pestle (Kimble Chase, Vineland, NJ) in an Eppendorf tube containing 50µl of 1X PBS. Based on morphology and movement, the parasite load and the percent metacyclics per midgut were determined using a hemocytometer.

**Transmission of *L. donovani* via sand fly bites**—Mice were anesthetized by intraperitoneal administration of ketamine (100mg/kg) with xylazine (10mg/kg). Upon full sedation, LubriFresh ophthalmic ointment (Major Pharmaceuticals) was topically applied to the eyes to prevent corneal dryness. Twenty flies with mature infections were applied either to the left ear of each mouse in experiments involving follow-up of the infection or to both ears for 3–18h time points, using vials with a meshed surface held in place by custom-made clamps. Sand flies were allowed to feed for 2–3h in the dark. Time to analysis was counted starting at midpoint of the exposure to sand flies. Five of 292 ears subjected to bites throughout the study had no evidence of transmission (no fed flies and no signs of probing on the ear) and were excluded from further analyses. For experiments involving follow-up of the course of infection, mice were monitored daily for appearance, level of activity, swelling, pain and ulceration during the course of infection.

**Scoring of blood-fed sand flies**—The percent of blood-fed flies was established for each mouse. The flies were aspirated from vials, anesthetized with CO<sub>2</sub>, washed in 5% soap solution, rinsed, and placed in 1X PBS. The number of blood-fed flies was determined by observing them under a stereomicroscope. In the absence of a visible blood meal in any of the sand flies subjected to a single ear, midguts were dissected and inspected microscopically for traces of blood.

**Preparation of sand fly salivary gland homogenate**—Salivary glands were dissected from five- to seven-day old female *Lu. longipalpis* sand flies, sonicated for 3–4 cycles and with one minute on ice in between, then centrifuged at 12,000×g for five minutes. The supernatant was collected and used immediately. One gland equivalent of the homogenate was mixed with the metacyclic parasite inoculum for each injection.

**Infection of mice by needle injection**—*L. donovani* amastigotes used in sand fly infections were cultured in Schneider's medium (Sigma) supplemented with 20% of inactivated FBS, 2mM L-glutamine, 100 units/ml penicillin, and 100µl/ml streptomycin. After seven to nine days, metacyclic parasites were purified from culture using a Ficoll (Sigma) gradient procedure as described previously (Späth and Beverley, 2001). The left ear of each mouse was injected intradermally with 10<sup>5</sup> metacyclics of *L. donovani* in a volume of 10µl in the absence or presence of an extract of one freshly prepared salivary gland using a 29-gauge needle.

**ELISA, Western blot and co-immunoprecipitation analyses**—Six hours after sand fly bites, exposed mice ears were harvested and homogenized in Procarta cell lysis buffer (eBioscience) using MagNA Lyser Green Beads (Roche). Tissue was further cleaned by passing through QIAshredder (Qiagen) and gDNA Eliminator (RNeasy Plus Mini Kits, Qiagen) columns. IL1β levels were measured directly from ear lysates using Mouse IL1β ELISA Ready-SET-GO! kits (eBioscience). For co-immunoprecipitation, equal amounts of protein from each sample (150µg) were incubated overnight at 4°C with 1µg of anti-ASC antibody (N-15-R; Santa Cruz Biotech, cat# sc-22514-R), followed by a 4h incubation period at 4°C with Pierce Protein A/G-agarose beads (Thermo Scientific). Beads were washed three times and heated for five minutes at 95°C with 2× reducing sample buffer

(Bio-Rad) and the eluted samples were run in 10% Mini-PROTEAN TGX pre-cast gels (Bio-Rad). For Western blot analyses, protein concentrations were measured from homogenized tissue lysates, and 35µg of protein from each sample was run in 10% Mini-PROTEAN TGX pre-cast gels (Bio-Rad). All electrophoresed gels were transferred onto PVDF membranes using Trans-Blot Turbo Transfer System (Bio-Rad), and membranes were blocked with 5% NFD milk in 1× PBS-Tween 20 (0.1%). Immunoblotting was performed using antibodies specific to IL1β (R&D, cat# AF-401-NA; 1:700), caspase-1 p-10 (M-20; Santa Cruz Biotech, cat# sc-514; 1:200), NLRP3 (Adipogen, cat# AG-20B-0006-C100; 1:1000), ASC (N-15-R; Santa Cruz Biotech, cat# sc-22514-R; 1:200) and β-actin (abcam cat# ab20272; 1:5000) antibodies; further immunolabeling was done using donkey anti-goat (Santa Cruz Biotech, cat# sc-2056; 1:3000), goat anti-rabbit (Jackson ImmunoResearch Laboratories, cat# 111-035-045; 1:3000), and goat anti-mouse (Jackson ImmunoResearch Laboratories, cat# 115-035-068; 1:3000) antibodies. Each blot was developed with SuperSignal West Femto Maximum Sensitivity Substrate (Thermo Scientific), and visualized using FluorChem<sup>®</sup> Q (Alpha Innotech). Exposure times for each Western blot varied between 10 to 30 seconds. Captured images were processed and analyzed using Photoshop CS4 (Adobe, Inc.).

For Western blots and co-immunoprecipitation assays, band densities were measured using ImageJ Software (NIH). Thereafter, the NLRP3, pro-IL-1β, pro-Caspase 1 and cleaved Caspase band densities were normalized to either actin or ASC band densities (Tables S1).

**Flow cytometry of ear tissue cells**—Ear pinna dermal sheets were harvested, treated with ethanol, separated using forceps and digested in PBS containing Liberase TL (Roche) at 37°C for 1 h. Digested tissues were homogenized in a tissue homogenizer (Medimachine; BD biosciences) and filtered in a 50 µm strainer. The resulting single cell suspensions were stained for Ly6C (clone AL-21; FITC; BD), Ly6G (clone 1A8; PE; BD), CD11b (clone M1/70; PE-Cy7; BD), and with the Fixable Yellow Dead Cell Stain Kit (Invitrogen), after being incubated with anti-Fc (CD16/32) antibodies to block unspecific binding for 30 min. For intracellular detection of IL-1β, ear cells were blocked and stained with surface markers as mentioned above. Thereafter, cells were fixed and permeabilized with Cytofix/Cytoperm (BD), followed by incubation with anti-mouse IL-1β proform antibody (clone NJTEN3, APC; eBioscience). Data were analyzed on a MACSQuant flow cytometer (Miltenyi Biotec). Cells were acquired based on forward and side scatter and data analyzed with FlowJo Software 4.3.

**In vivo blocking of IL1β**—Twenty milligrams of Anakinra (Kineret; Amgen) or PBS was administered to mice by intra-peritoneal injection 12h and immediately before transmission by infected sand flies. Mice were euthanized at 6h post-transmission to assess infiltration of neutrophils into the ears, and at three weeks post-transmission to determine the parasite burden in draining lymph nodes and spleens. Anakinra was kindly provided by Dr. Raphaela Goldbach-Mansky (National Institute of Arthritis and Musculoskeletal and Skin Diseases, National Institute of Health).

**In vitro measurement of IL1β and IL-10 in cultures of bone-marrow-derived macrophages (BMDM)**—Bone marrow cells were isolated from the femurs and tibiae of

BALB/c mice. Cells were cultured with RPMI medium containing 10% of fetal bovine serum (FBS) along with 20 ng/ml of M-CSF for 7 days. Some wells containing BMDMs were treated with 500 ng/ml of LPS (Sigma). After 4 h of stimulation cells were washed with RPMI, and infected with stationary-phase *L. donovani* promastigotes in two different ratios 1:5 and 1:10 (BMDM: Parasites). After 6 h of incubation cell supernatants were collected and centrifuged to remove parasites. IL1 $\beta$  (Mouse IL-1 beta ELISA Ready-SET-GO!<sup>®</sup>, Cat No 88-7013, eBioscience) and IL-10 (Mouse IL-10 ELISA Ready-SET-GO!<sup>®</sup>, Cat No 88-7105, eBioscience) cytokine levels were measured according to manufacturer's instructions.

***In vitro* invasion of BMDM by gut-residing parasites**—BMDMs were prepared as described above. After 7 days, cells were infected with *L. donovani* metacyclic parasites isolated from different groups of infected sand flies at a ratio of 1:10 (BMDM: Parasites). After 48 h of infection cells were washed, fixed with alcohol, and stained with Giemsa. Intracellular parasite numbers were counted in 300–400 macrophages to calculate the percentage of macrophages that were infected by parasites and the mean number of parasites/infected macrophage.

**Parasite load determination by quantitative PCR**—Immediately after transmission by infected sand flies, mice ears were cut and lysed for DNA purification using DNeasy Blood & Tissue kits (Qiagen). Seventy-five nanograms of sample DNA was used as a template in a Taqman-based quantitative PCR. The target DNA was amplified from a kinetoplast minicircle DNA of the parasite. The sequence of primers is given in the Key Resource Table, with the addition of a fluorescent probe 5'-RAAARKKVRTRCA GAAAYCCCGT-3' for detection. A Black Hole Quencher moiety is coupled to the 3' end and Calfluor Red is coupled to a C6 linker at the 5' end. The degenerate letter code is according to the Nomenclature Committee of the International Union of Biochemistry (<http://www.chem.qmul.ac.uk/iubmb/misc/naseq.html>). The fluorescent probe is added to the reaction mixture at a final concentration of 1.5 pmols/ $\mu$ L. Cycling parameters: preheat at 95°C for 180 seconds and then 40 two-step cycles of 95°C for 10 seconds and 55°C for 30 seconds. To evaluate the number of *Leishmania* cells that were represented by a given cycle threshold (Ct) value, a standard curve was constructed by purification of DNA from naïve mice ears spiked with a known number of parasites (Figure S1B).

**Parasite load determination by serial dilution**—Mice were euthanized by CO<sub>2</sub> inhalation. The spleen and the lymph node draining the bite sites were removed from each mouse under aseptic conditions. The lymph node was macerated in an Eppendorf tube containing 200  $\mu$ L of complete Schneider's medium. The spleen was cut into small pieces, transferred to a 70  $\mu$ m cell strainer and macerated in 1 mL of complete Schneider's medium using the back of a syringe plunger. The parasite burden was quantified from the macerate by limiting dilution assays where the number of viable *Leishmania* parasites in each lymph node or spleen was determined from the highest dilution at which *Leishmania* promastigotes could be grown after 15 days of incubation at 26°C.

**Reverse-transcriptase quantitative PCR**—Mice were euthanized at indicated time points after exposure to infected sand flies, non-infected sand flies, or after needle injection. The whole ear was homogenized using MagNA Lyser Green Beads (Roche) and total RNA was extracted using PureLink RNA Mini kits (Ambion). Five hundred nanograms of total RNA was reverse-transcribed into cDNA using random hexamers with the Taqman High-Capacity cDNA Reverse Transcription kit (Life Technologies). Expression of the genes listed in Table S2 was determined using Taqman Gene Expression assays (Applied Biosystems) in the CFX96 Touch Real-Time System (BioRad, Hercules, CA). Expression values were determined by the  $2^{-Ct}$  method; samples were normalized to GAPDH expression and determined relative to expression values from naïve mice.

**Immunohistochemical and TUNEL staining of ear tissue**—Mouse ears were fixed in 10% buffered formalin phosphate solution and paraffin embedded according to standard procedures. Slides of consecutive serial sections of bites sites were prepared for immune staining. Paraffin sections were dewaxed and rehydrated prior to staining. Dewaxed sections were incubated with anti-Ly6G antibody, clone RB6-8C5 (Thermo Fisher Scientific, 1:100) for neutrophil staining; anti-macrophage antibody, clone MAC387 (abcam, 1:100); anti-IL1 $\beta$  antibody conjugated with HRP (abcam, cat# ab106035; 1:100) for mature IL1 $\beta$  staining; and the corresponding isotype control antibody for each analyte. All stained sections were counterstained with Hematoxylin. For mast cell staining, dewaxed slides were stained with alcian blue counterstained with safranin. TUNEL reactions were performed on paraffin sections that were dewaxed and rehydrated. Slides were incubated with Tdt, UTP and terminal transferase buffer, washed, and incubated with anti-Dig. Color was developed with Fuchsin and slides were counterstained with Hematoxylin. All of the histochemical and immunohistochemical staining was done by Histoserv Inc, Gaithersburg, MD, USA. Stained sections were analyzed at the Infectious Disease Pathogenesis Section (IDPS), Comparative Medicine Branch (CMB), Division of Intramural Research (DIR), NIAID/ NIH, using an Olympus BX51 microscope. Images were taken with an Olympus DP73 Camera using Olympus cellSens Dimension ver.1.9 software. Mast cell counts were performed using the Keyence BZ-9000 microscope and analyzed with BZ-II Viewer software.

**Exposure of infected flies to LB/Agar**—Twenty *Lu. longipalpis* sand flies with mature transmissible infections were placed in a custom-made feeder with a meshed surface to provide access to sterile LB/Agar plates (Sigma-Aldridge). The meshes were autoclaved whereas the feeders were sterilized overnight in 70% ethanol and left to dry for at least 30 minutes inside a laminar flow hood where the probing experiments were carried out. The LB/Agar plates were placed on top of each feeder for 2h and were kept warm throughout the experiment by a heating device (SunBeam, Model 828B). The plates were then incubated at 30°C and 5% CO<sub>2</sub> for 24–48h.

**Plating of midgut microbiota**—Depending on the experiment, up to 30 sand fly guts were dissected, washed three times in sterile PBS and macerated with a plastic pestle in 450 $\mu$ l of PBS. The equivalent of 10 guts in 150 $\mu$ l were plated on LB agar plates (KD Medical). The plates were incubated at 28°C for 24–48h.

**Amplification, cloning and sequence identification of bacterial DNA**—Colonies growing in LB/agar plates after exposure to infected sand flies were picked with a sterile pipet tip and transferred to 30uL of sterile molecular biology grade water. An aliquot was transferred to Luria broth (LB) and bacteria was incubated at 28°C overnight and a glycerol stock was prepared from the culture and stored at -70°C. Water containing the bacteria (5 µl) was used as a DNA template for a PCR reaction using 16S PCR primers (16S\_27 forward primer: 5'-AGA GTT TGA TCC TGG CTC AG-3') and 16S\_27 reverse primer: 5'-GGT TAC CTT GTT ACG ACT T-3'), Taq DNA Polymerase (New England BioLabs), 10mM dNTP Mix (Promega) and Molecular Biology Grade Water (Corning). PCR conditions started with denaturation at 95°C for 5 minutes followed by 35 cycles of denaturation at 95°C for 1 minute, annealing at 55°C for 1 minute, and extension at 72°C for 1min. Final extension at 72°C was allowed to run for 10 minutes. Amplicons were visualized by gel electrophoresis with a 1.5% agarose gel (UltraPure™ Agarose - invitrogen) in 1X TAE buffer (Quality Biological). The PCR product was cloned directly into the PCR4-TOPO Vector (ThermoFisher Scientific) following manufacturing specifications. Plasmids of positive clones were isolated using the GeneJet Plasmid Miniprep Kit (Thermo Scientific) and sequenced at Eurofins MWG Operon using M13 Forward and M13 Reverse primers. Sequences were analyzed using the DNASTAR package (Lasergene) and identified using the NCBI blastn.

**Infection of mice by co-injection of *Leishmania* and live bacteria or LPS**—Mice ears were co-injected intradermally with 10<sup>5</sup> metacyclics of *L. donovani* and 10<sup>3</sup> live *Solibacillus* bacteria or 1µg of LPS in a total volume of 10µl. After identification of *Solibacillus* from a *Leishmania*-positive egestion bite site, the agar bacterial colony was transferred to 30uL of sterile molecular biology grade water. An aliquot was transferred to LB and grown overnight at 28°C and an aliquot was stored as a glycerol stock. A sample of the bacteria was sequenced to confirm the identity of *Solibacillus* and to ensure that it was the only species present in the preparation. Further, a standard curve was established for the number of bacteria by counting colonies plated at various dilutions and optical densities (ODs). For co-injection, *Solibacillus* was grown in Luria broth overnight at 28°C. On the day of injection, 100µl of bacteria was inoculated into 5ml of fresh Luria broth and growth was monitored hourly until it reached an OD<sub>600nm</sub> of 0.15. The culture was then diluted with LB medium according to the predetermined standard curve to give 10<sup>3</sup> cfu per 5µl. As for LPS (Lipopolysaccharides from *Escherichia coli* O26:B6, Sigma), the stock solution (2mg/ml) was diluted to 200µg/ml immediately before use. For co-injection, 5µl containing 10<sup>5</sup> *L. donovani* metacyclics was mixed with 5µl of either 10<sup>3</sup> live *Solibacillus* bacteria or 1µg of LPS.

## QUANTIFICATION AND STATISTICAL ANALYSIS

**Samples Sizes**—n represents the number of mice, mice ears or sand flies as described in legends of each figure.

**Statistical Analysis**—Data of parasite numbers are portrayed as geometric means with 95% CI; all other data are portrayed as means with SEM or SD. As parasite numbers in the ear of mice transmitted by infected sand flies bites do not follow a Gaussian distribution, we

used the stratified Wilcoxon rank sum test to measure significance values from any data related to splenic parasite burden. To compare multiple groups, one-way ANOVA followed by a Holm-Sidak multiple comparisons test was performed. To compare the number of neutrophils in the ear after IS compared to resting skin, we used the Mann-Whitney test. All other significance values were determined using the two-tailed student's *t*-test. Statistical tests were performed using GraphPad Prism 5.0 software.

## Supplementary Material

Refer to Web version on PubMed Central for supplementary material.

## Acknowledgments

We thank Jose M.C. Ribeiro (NIAID, NIH) and Claudia Brodskyn (CNPq/FIOCRUZ) for critical review of the manuscript. We are also grateful to Zhen Jiang (CBER, FDA) for help with statistical analysis. This work was funded by the Intramural Research Programs at the NIAID, NIH, and by CBER, FDA, USA. FDA authors' contributions represent their best judgment and do not bind or obligate FDA.

## References

- Abdeladhim M, Kamhawi S, Valenzuela JG. What's behind a sand fly bite? The profound effect of sand fly saliva on host hemostasis, inflammation and immunity. *Infect Genet Evol.* 2014; 28:691–703. [PubMed: 25117872]
- Afonina IS, Muller C, Martin SJ, Beyaert R. Proteolytic Processing of Interleukin-1 Family Cytokines: Variations on a Common Theme. *Immunity.* 2015; 42:991–1004. [PubMed: 26084020]
- Atayde VD, Aslan H, Townsend S, Hassani K, Kamhawi S, Olivier M. Exosome Secretion by the Parasitic Protozoan *Leishmania* within the Sand Fly Midgut. *Cell Rep.* 2015; 13:957–967. [PubMed: 26565909]
- Berggoetz M, Schmid M, Ston D, Wyss V, Chevillon C, Pretorius AM, Gern L. Protozoan and bacterial pathogens in tick salivary glands in wild and domestic animal environments in South Africa. *Ticks Tick Borne Dis.* 2014; 5:176–185. [PubMed: 24378080]
- Bradley LM, Douglass MF, Chatterjee D, Akira S, Baaten BJ. Matrix metalloprotease 9 mediates neutrophil migration into the airways in response to influenza virus-induced toll-like receptor signaling. *PLoS Pathog.* 2012; 8:e1002641. [PubMed: 22496659]
- Charmoy M, Hurrell BP, Romano A, Lee SH, Ribeiro-Gomes F, Riteau N, Mayer-Barber K, Tacchini-Cottier F, Sacks DL. The Nlrp3 inflammasome, IL-1beta, and neutrophil recruitment are required for susceptibility to a non-healing strain of *Leishmania major* in C57BL/6 mice. *Eur J Immunol.* 2015
- Chiba N, Shimada K, Chen S, Jones HD, Alsabeh R, Slepkin AV, Peterson E, Crother TR, Arditi M. Mast cells play an important role in chlamydia pneumoniae lung infection by facilitating immune cell recruitment into the airway. *J Immunol.* 2015; 194:3840–3851. [PubMed: 25754739]
- Cox J, Mota J, Sukupolvi-Petty S, Diamond MS, Rico-Hesse R. Mosquito bite delivery of dengue virus enhances immunogenicity and pathogenesis in humanized mice. *J Virol.* 2012; 86:7637–7649. [PubMed: 22573866]
- De Filippo K, Dudeck A, Hasenberg M, Nye E, van Rooijen N, Hartmann K, Gunzer M, Roers A, Hogg N. Mast cell and macrophage chemokines CXCL1/CXCL2 control the early stage of neutrophil recruitment during tissue inflammation. *Blood.* 2013; 121:4930–4937. [PubMed: 23645836]
- de Oliveira S, Rosowski EE, Huttenlocher A. Neutrophil migration in infection and wound repair: going forward in reverse. *Nat Rev Immunol.* 2016; 16:378–391. [PubMed: 27231052]
- Gomes R, Oliveira F. The immune response to sand fly salivary proteins and its influence on leishmania immunity. *Front Immunol.* 2012; 3:110. [PubMed: 22593758]

- Guarda G, Braun M, Staehli F, Tardivel A, Mattmann C, Forster I, Farlik M, Decker T, Du Pasquier RA, Romero P, Tschopp J. Type I interferon inhibits interleukin-1 production and inflammasome activation. *Immunity*. 2011; 34:213–223. [PubMed: 21349431]
- Guo H, Callaway JB, Ting JP. Inflammasomes: mechanism of action, role in disease, and therapeutics. *Nat Med*. 2015; 21:677–687. [PubMed: 26121197]
- Gurung P, Karki R, Vogel P, Watanabe M, Bix M, Lamkanfi M, Kanneganti TD. An NLRP3 inflammasome-triggered Th2-biased adaptive immune response promotes leishmaniasis. *J Clin Invest*. 2015; 125:1329–1338. [PubMed: 25689249]
- Kelly PH, Bahr SM, Serafim TD, Ajami NJ, Petrosino JF, Meneses C, Kirby JR, Valenzuela JG, Kamhawi S, Wilson ME. The Gut Microbiome of the Vector *Lutzomyia longipalpis* Is Essential for Survival of *Leishmania infantum*. *MBio*. 2017; 8
- Lawyer, PG., Meneses, C., Rowland, T., Rowton, ED. Care and maintenance of phlebotomine sand flies. Walter Reed Army Institute of Research and BEI Resources; Bethesda, Maryland: 2016. p. 62
- Lima-Junior DS, Costa DL, Carregaro V, Cunha LD, Silva AL, Mineo TW, Gutierrez FR, Bellio M, Bortoluci KR, Flavell RA, et al. Inflammasome-derived IL-1 $\beta$  production induces nitric oxide-mediated resistance to *Leishmania*. *Nat Med*. 2013; 19:909–915. [PubMed: 23749230]
- Liu XY, Bonnet SI. Hard tick factors implicated in pathogen transmission. *PLoS Negl Trop Dis*. 2014; 8:e2566. [PubMed: 24498444]
- Monteiro CC, Villegas LE, Campolina TB, Pires AC, Miranda JC, Pimenta PF, Secundino NF. Bacterial diversity of the American sand fly *Lutzomyia intermedia* using highthroughput metagenomic sequencing. *Parasit Vectors*. 2016; 9:480. [PubMed: 27581188]
- Murray PJ, Wynn TA. Protective and pathogenic functions of macrophage subsets. *Nat Rev Immunol*. 2011; 11:723–737. [PubMed: 21997792]
- Opendakker G, Van den Steen PE, Dubois B, Nelissen I, Van Coillie E, Masure S, Proost P, Van Damme J. Gelatinase B functions as regulator and effector in leukocyte biology. *J Leukoc Biol*. 2001; 69:851–859. [PubMed: 11404367]
- Peters NC, Egen JG, Secundino N, Debrabant A, Kimblin N, Kamhawi S, Lawyer P, Fay MP, Germain RN, Sacks D. In vivo imaging reveals an essential role for neutrophils in leishmaniasis transmitted by sand flies. *Science*. 2008; 321:970–974. [PubMed: 18703742]
- Peters NC, Kimblin N, Secundino N, Kamhawi S, Lawyer P, Sacks DL. Vector transmission of leishmania abrogates vaccine-induced protective immunity. *PLoS Pathog*. 2009; 5:e1000484. [PubMed: 19543375]
- Pingen M, Bryden SR, Pondeville E, Schnettler E, Kohl A, Merits A, Fazakerley JK, Graham GJ, McKimmie CS. Host Inflammatory Response to Mosquito Bites Enhances the Severity of Arbovirus Infection. *Immunity*. 2016; 44:1455–1469. [PubMed: 27332734]
- Porta C, Rimoldi M, Raes G, Brys L, Ghezzi P, Di Liberto D, Dieli F, Ghisletti S, Natoli G, De Baetselier P, et al. Tolerance and M2 (alternative) macrophage polarization are related processes orchestrated by p50 nuclear factor kappaB. *Proc Natl Acad Sci U S A*. 2009; 106:14978–14983. [PubMed: 19706447]
- Qiu Y, Nakao R, Ohnuma A, Kawamori F, Sugimoto C. Microbial population analysis of the salivary glands of ticks; a possible strategy for the surveillance of bacterial pathogens. *PLoS One*. 2014; 9:e103961. [PubMed: 25089898]
- Radwan M, Stiefvater R, Grunert T, Sharif O, Miller I, Marchetti-Deschmann M, Allmaier G, Gemeiner M, Knapp S, Kovarik P, et al. Tyrosine kinase 2 controls IL-1 $\beta$  production at the translational level. *J Immunol*. 2010; 185:3544–3553. [PubMed: 20713887]
- Ribeiro-Gomes FL, Sacks D. The influence of early neutrophil-*Leishmania* interactions on the host immune response to infection. *Front Cell Infect Microbiol*. 2012; 2:59. [PubMed: 22919650]
- Rogers ME. The role of leishmania proteophosphoglycans in sand fly transmission and infection of the Mammalian host. *Front Microbiol*. 2012; 3:223. [PubMed: 22754550]
- Sant'Anna MR, Darby AC, Brazil RP, Montoya-Lerma J, Dillon VM, Bates PA, Dillon RJ. Investigation of the bacterial communities associated with females of *Lutzomyia* sand fly species from South America. *PLoS One*. 2012; 7:e42531. [PubMed: 22880020]



- Schmid MA, Glasner DR, Shah S, Michlmayr D, Kramer LD, Harris E. Mosquito Saliva Increases Endothelial Permeability in the Skin, Immune Cell Migration, and Dengue Pathogenesis during Antibody-Dependent Enhancement. *PLoS Pathog.* 2016; 12:e1005676. [PubMed: 27310141]
- Sharma P, Sharma S, Maurya RK, Das De T, Thomas T, Lata S, Singh N, Pandey KC, Valecha N, Dixit R. Salivary glands harbor more diverse microbial communities than gut in *Anopheles culicifacies*. *Parasit Vectors.* 2014; 7:235. [PubMed: 24886293]
- Shi C, Pamer EG. Monocyte recruitment during infection and inflammation. *Nat Rev Immunol.* 2011; 11:762–774. [PubMed: 21984070]
- Shimada K, Crother TR, Karlin J, Dagvadorj J, Chiba N, Chen S, Ramanujan VK, Wolf AJ, Vergnes L, Ojcius DM, et al. Oxidized mitochondrial DNA activates the NLRP3 inflammasome during apoptosis. *Immunity.* 2012; 36:401–414. [PubMed: 22342844]
- Sica A, Invernizzi P, Mantovani A. Macrophage plasticity and polarization in liver homeostasis and pathology. *Hepatology.* 2014; 59:2034–2042. [PubMed: 24115204]
- Silverman JM, Reiner NE. *Leishmania* exosomes deliver preemptive strikes to create an environment permissive for early infection. *Front Cell Infect Microbiol.* 2011; 1:26. [PubMed: 22919591]
- Späth GF, Beverley SM. A lipophosphoglycan-independent method for isolation of infective *Leishmania* metacyclic promastigotes by density gradient centrifugation. *Exp. Parasitol.* 2001; 99:97–103. [PubMed: 11748963]
- Tchioffo MT, Boissiere A, Abate L, Nsango SE, Bayibeki AN, Awono-Ambene PH, Christen R, Gimonneau G, Morlais I. Dynamics of Bacterial Community Composition in the Malaria Mosquito's Epithelia. *Front Microbiol.* 2015; 6:1500. [PubMed: 26779155]
- WHO. A global brief on vector-borne diseases. 2014.

### Highlights

- Gut microbiota egested by *Leishmania*-infected sand flies prime the host inflammasome
- Inflammasome-derived IL-1 $\beta$  sustains recruitment of neutrophils to bite sites
- Giving antibiotics to sand flies before transmission abolishes neutrophil infiltration
- Abolishing neutrophil infiltration at bite sites impairs *Leishmania* dissemination

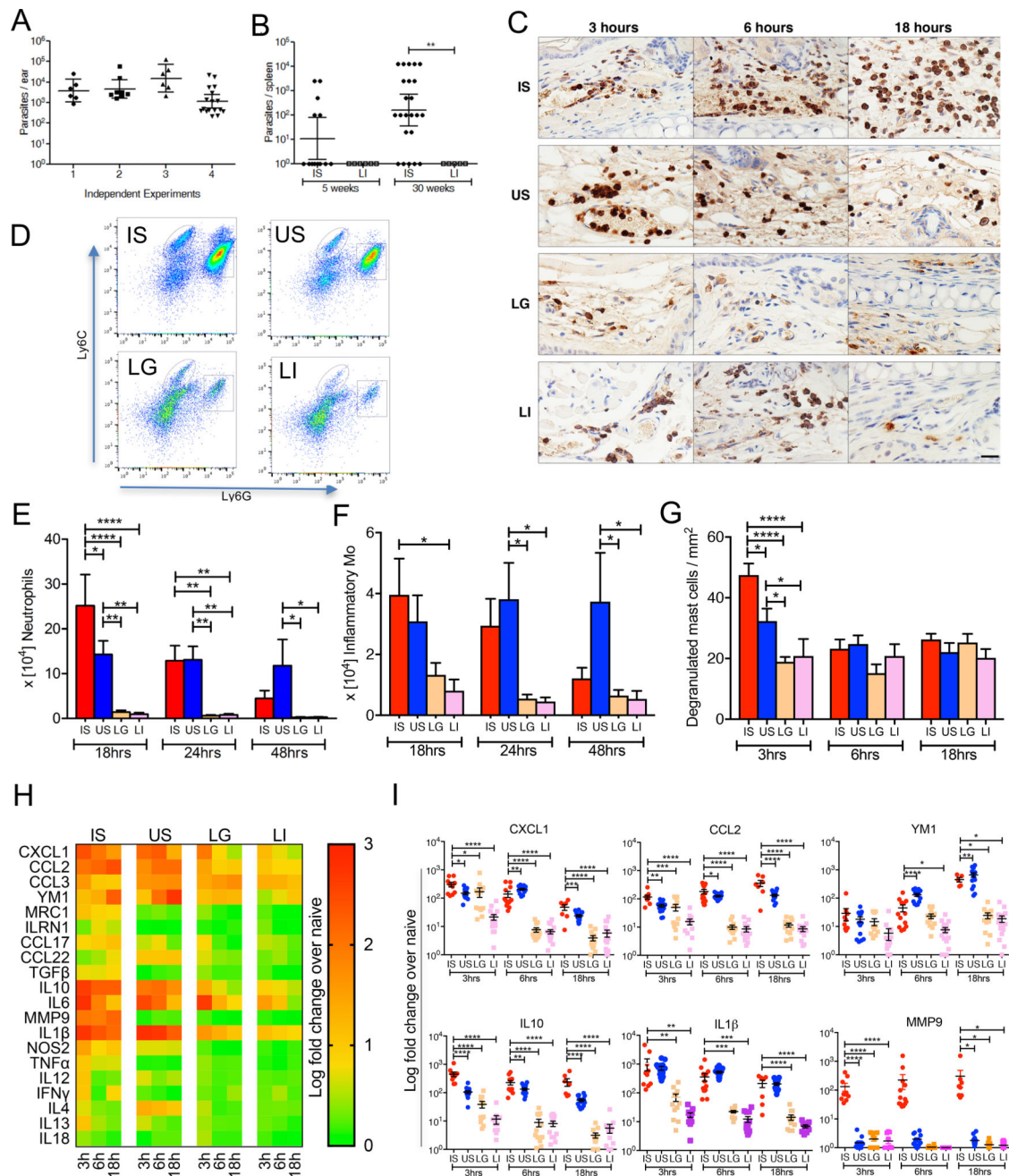


**Figure 1. The inflammatory response at the bite site of vector-transmitted *L. donovani* parasites**  
 (A) Parasite burden determined by qPCR in individual mice ears 3h after exposure to 20 infected sand flies (n = 6 mice ears per experiment).  
 (B) Parasite burden in individual mice spleens was determined by serial dilution at five and 30 weeks after exposure to 20 infected sand flies (IS) belonging to the same group or to an intradermal injection of 10<sup>5</sup> metacyclic parasites (LI). Data are pooled from two independent experiments (n = 13 for IS, and 5 mice for LI).  
 (C–I) Mice ears 3–48h after exposure to 20 IS, 20 uninfected sand flies (US), intradermal co-inoculation with LI plus extract of one salivary gland (LG), and LI.

(C) Mice ear sections stained with anti-Gr1 antibody. Pictures are representative of four independent experiments (n = 4 mice ears per condition per timepoint). Scale bar indicate 20 $\mu$ m.

(D–F) Cells recovered from individual mice ears were stained for flow cytometry. Data are representative of two independent experiments (n = 6 mice ears per condition per timepoint).

(D) Representative plots of Ly6G and Ly6C expression distinguish neutrophils (square gate) and inflammatory monocytes (oval gate) graphed in (E) and (F), respectively.

(G) Degranulated mast cells in at least six fields counted from ear sections stained with Toluidine blue. Data are representative of four independent experiments (n = 5 mice ears per condition per timepoint).

(H and I) mRNA expression of inflammatory mediators produced in mice ears determined by qPCR. Data are pooled from more than three independent experiments (n = 7 mice ears per condition per timepoint).

(H) Heat map of the global inflammatory skin response.

(I) Expression profile of distinct genes relevant to the inflammatory response after IS.

Statistical significance \* $P < 0.05$ ; \*\* $P < 0.01$ ; \*\*\* $P < 0.001$ , \*\*\*\* $P < 0.0001$  was calculated using the Wilcoxon ranked sum test (A and B), the one-way ANOVA followed by a Holm-Sidak multiple comparisons test (E–G and I). Error bars in (A, B) indicate the geometric mean with 95% CI. Error bars in (E–G and I) indicate the mean  $\pm$  SEM.

See also Figure S1, S2 and S3.

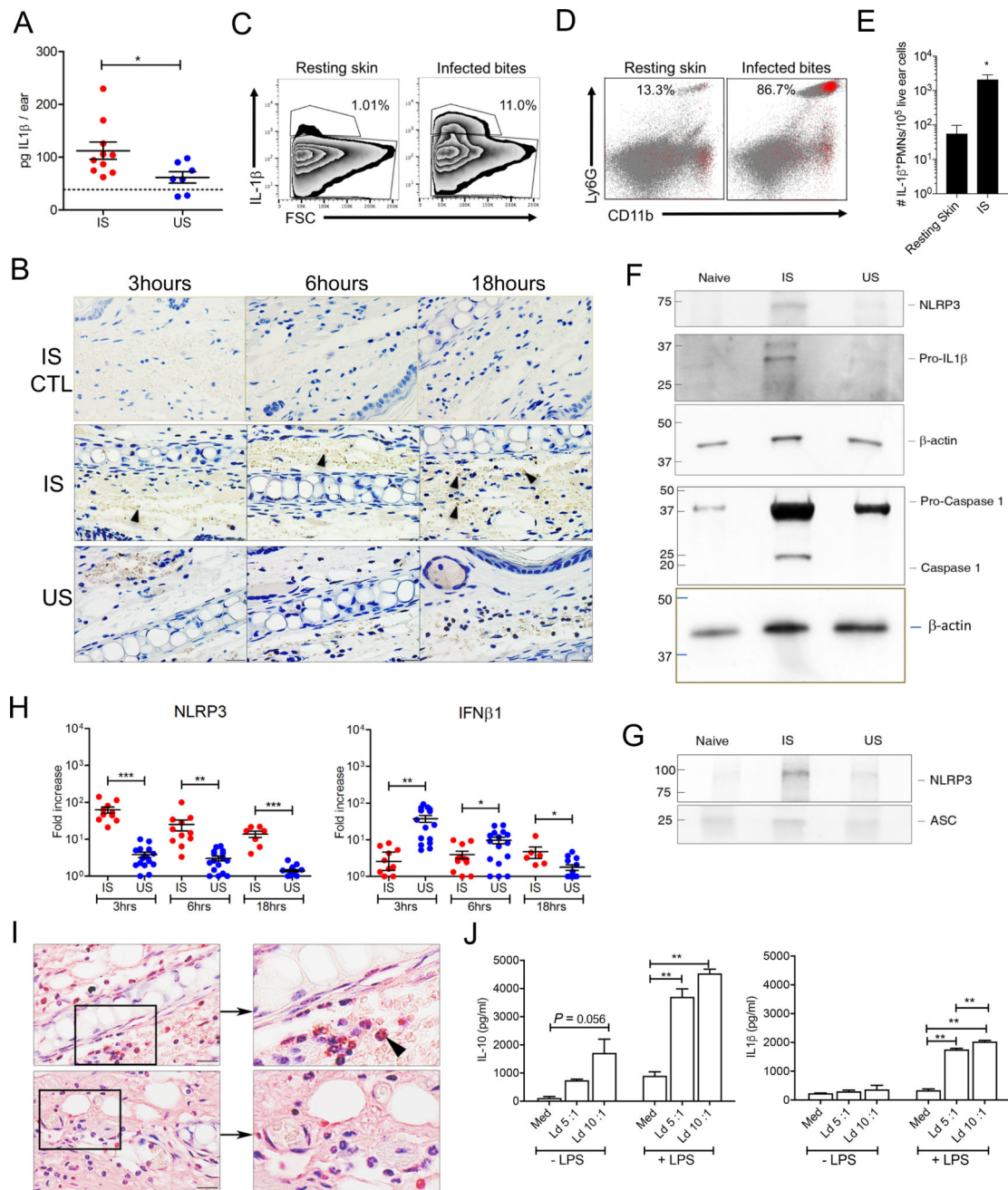


**Figure 2. *L. donovani*-infected sand fly bites activate the NLRP3 inflammasome in neutrophils** (A, C–G and I) Mice ears processed 6h after exposure to 20 infected (IS) or uninfected (US) sand flies.

(A) Ex-vivo IL1 $\beta$  protein levels from ear lysates measured by ELISA. Data are representative of two independent experiments (n = 7 mice ears per condition). Dotted line represents the mean + SEM of endogenous IL1 $\beta$  levels in naïve samples.

(B) Mice ear sections stained with either anti-IL1 $\beta$  antibody targeting the mature protein or its isotype control (CTL) at 3–18h after IS or US. Pictures are representative of two

independent experiments (n = 2 mice ears per condition per timepoint). Scale bars indicate 20 $\mu$ m. Arrows indicate IL1 $\beta$  secreting cells.

(C–E) Cells recovered from mice ears after IS were stained for flow cytometry. Representative plots of IL1 $\beta$ <sup>+</sup> cells (C) back-gated (red) onto LY6G<sup>+</sup> / CD11b<sup>+</sup> neutrophils (D). (E) The number of IL1 $\beta$ <sup>+</sup> neutrophils per 10<sup>5</sup> ear cells from two independent experiments (n = 6 mice ears per condition).

(F) Representative Western blot of NLRP3, Caspase 1 and IL1 $\beta$  protein levels after IS and US (n = 4 mice ears per condition).

(G) Representative Western blot of NLRP3 protein levels after immunoprecipitation using anti-ASC antibody (n = 2 mice ears per condition).

(H) NLRP3 and IFN $\beta$  mRNA expression determined by qPCR at 3–18h after IS or US. Data are pooled from three independent experiments (n = 7 mice ears per condition per timepoint).

(I) Mice ear sections stained with TUNEL. Pictures are representative of two independent experiments (n = 3 mice ears per condition). Boxed area is magnified to highlight apoptotic cells (arrow). Scale bars indicate 20 $\mu$ m.

(J) Mature IL1 $\beta$  and IL-10 cytokine levels in cell culture supernatant after *in vitro* stimulation of bone marrow-derived macrophages with *L. donovani* (Ld) stationary parasites in the presence or absence of lipopolysaccharide (LPS). Med, medium. Data are representative of two to three independent experiments (n = 2 replicates per condition). Statistical significance \**P* < 0.05, \*\**P* < 0.01, \*\*\**P* < 0.001 calculated by the unpaired two-tailed *t* test (A and H), the Mann-Whitney test (E), and the one-way ANOVA followed by a Holm-Sidak multiple comparisons test (J). Error bars indicate the mean  $\pm$  SEM. See also Table S1.

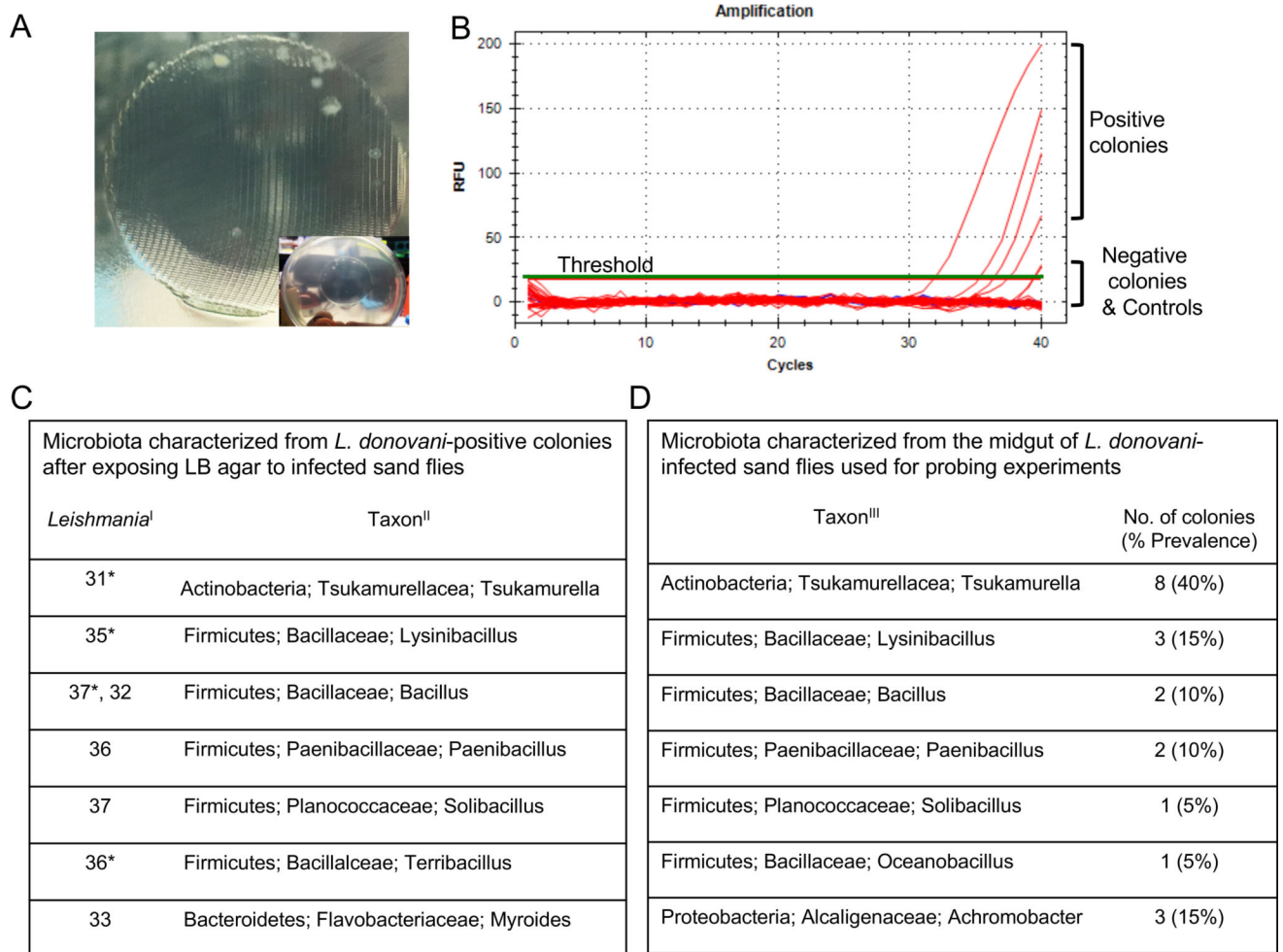


**Figure 3. Identification of gut microbes egested during infected sand fly bites**

(A) Bacterial colonies growing on LB/Agar after exposure to *L. donovani*-infected sand flies. Inset shows the mesh imprint of the feeder containing the sand flies. Pictures representative of five independent experiments.

(B) Representative Real-Time PCR amplification curves (red lines) for *Leishmania* minicircle kDNA using bacterial colonies picked from agar plates as template. Green line, Threshold. Blue Lines, Negative controls (water or agar).

(C) Bacteria identified from *Leishmania*-positive colonies. I, Real-time PCR  $C_T$  values for amplified *Leishmania*. II, Taxonomy of bacteria ordered by phylum, family, and genus. \*, colonies depicted in (B).

(D) Bacteria identified from the midgut of infected sand fly groups used in (A). III, Taxonomy of bacteria ordered by phylum, family, and genus.

See also Video S1.

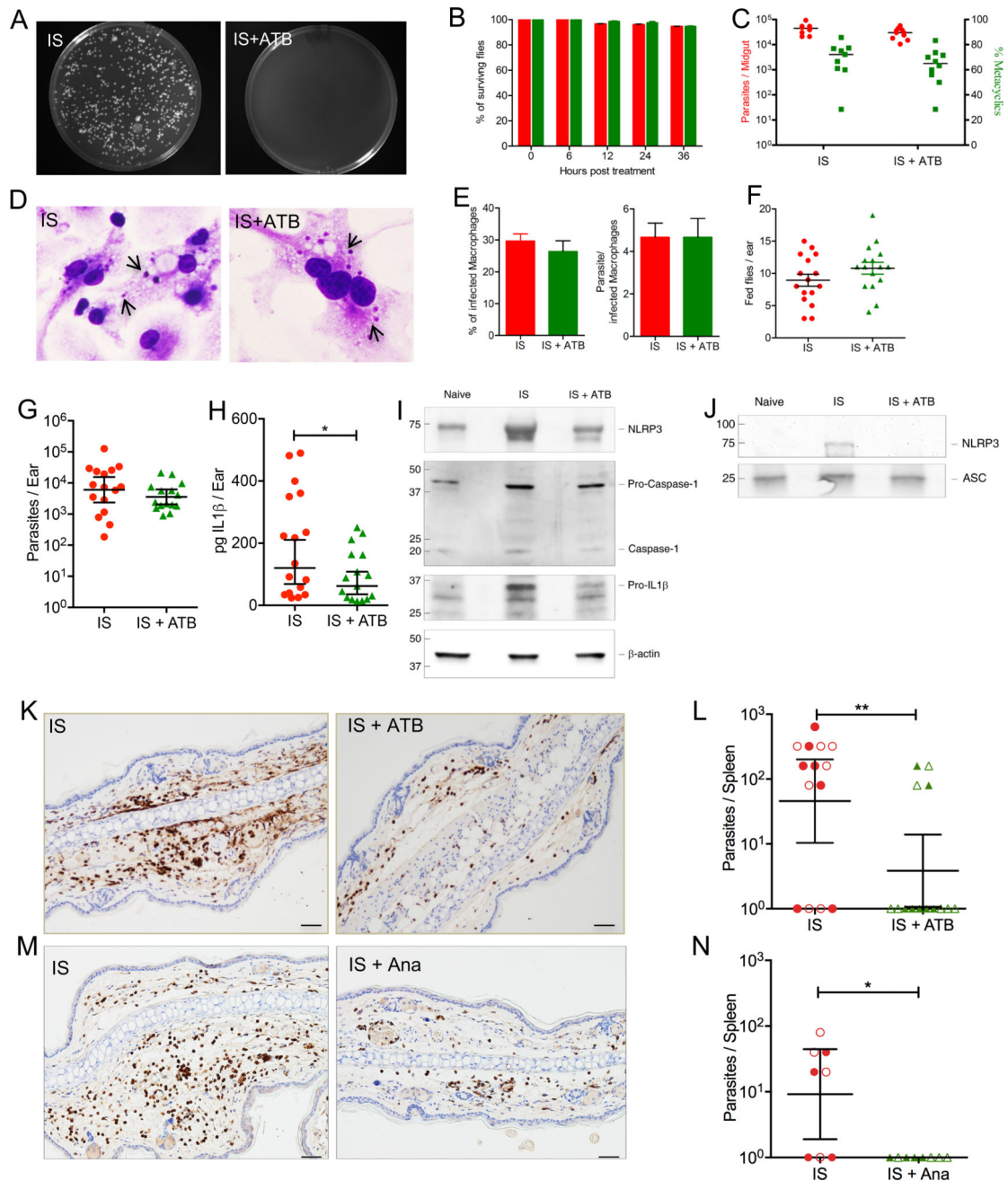


**Figure 4. Diminishing sand fly gut microbiota mitigates inflammasome activation, abrogates neutrophil recruitment and compromises dissemination of *Leishmania donovani***

(A–C and F–L) Sand flies harboring mature infections with *L. donovani* were left untreated (IS) or were provided a cocktail of three antibiotics for 36h prior to parasite transmission to mice ears (IS+ATB).

(A) Bacterial colony growth on LB/Agar after plating 10 midguts.

(B) Survival of sand flies without (red) and after antibiotic treatment (green).

(C) Parasite burden and percent metacyclics in sand flies prior to transmission.

(A–C) Data are representative of four independent experiments (n = 9 sand flies per condition per timepoint).



(D and E) *In vitro* invasion and multiplication of anterior gut residing parasites from IS or IS +ATB in bone marrow-derived macrophages (BMDM). Data are representative of two independent experiments.

(D) BMDM 48h after infection. Arrows indicate intracellular *Leishmania* amastigotes.

(E) Percent of infected BMDM and the number of parasites per cell.

(F) Feeding score after parasite transmission to mice ears. Data representative of four independent experiments (n = 16 sand flies per condition).

(G–J) Mice ear lysates after exposure to 20 IS or IS+ATB.

(G) Parasite burden determined by qPCR from individual mice ears 2h after bites.

(H) *Ex-vivo* IL1 $\beta$  protein levels measured by ELISA 6h after bites.

(G and H) Data are pooled from two independent experiments (n = 15 mice ears per condition).

(I) Representative Western blot of NLRP3, Caspase 1 and IL1 $\beta$  protein levels (n = 2 mice ears per condition).

(J) Representative Western blot of NLRP3 protein levels after immunoprecipitation using anti-ASC antibody (n = 2 mice ears per condition).

(K and L) Mice ears were exposed to IS or IS+ATB.

(M and N) Mice were left untreated or were treated with anakinra 12h and immediately before exposure to IS (IS+Ana).

(K and M) Mice ear sections stained with anti-Gr1 antibody 6h after exposure to IS. Data are representative of two independent experiments (n = 4–5 mice ears per condition). Scale bars indicate 50 $\mu$ m.

(L and N) Parasite burden in spleens of individual mice determined by serial dilution three weeks after exposure to IS or IS+ATB. Data are pooled from two independent experiments distinguished by solid and clear symbols (n = 8 mice per condition).

Statistical significance \* $P < 0.05$ , \*\* $P < 0.01$  was calculated using the unpaired two-tailed  $t$  test (H) and the Wilcoxon ranked sum test (L and N). Error bars indicate the geometric mean with 95% CI for parasite burden (C), (G), (L) and (N), and the mean  $\pm$  SEM for (B), percent metacyclics (C), (E), (F) and (H).

See also Figure S4 and Table S1.